Citation: CPT Pharmacometrics Syst. Pharmacol. (2020) 9, 617–627; doi:10.1002/psp4.12557

ARTICLE

Application of the Nested Enzyme-Within-Enterocyte (NEWE) Turnover Model for Predicting the Time Course of Pharmacodynamic Effects

Hiroyuki Takita[1,2], Adam S. Darwich[1,3], Amais Ahmad[1] and Amin Rostami-Hodjegan[1,4,*]

The gut wall consists of many biological elements, including enterocytes. Rapid turnover, a prominent feature of the enterocytes, has generally been ignored in the development of enterocyte-targeting drugs, although it has a comparable rate to other kinetic rates. Here, we investigated the impact of enterocyte turnover on the pharmacodynamics of enterocyte-targeting drugs by applying a model accounting for turnover of enterocytes and target proteins. Simulations showed that the pharmacodynamics depend on enterocyte lifespan when drug-target affinity is strong and half-life of target protein is long. Interindividual variability of enterocyte lifespan, which can be amplified by disease conditions, has a substantial impact on the variability of response. However, our comprehensive literature search showed that the enterocyte turnover causes a marginal impact on currently approved enterocyte-targeting drugs due to their relatively weak target affinities. This study proposes a model-informed drug development approach for selecting enterocyte-targeting drugs and their optimal dosage regimens.

Study Highlights

WHAT IS THE CURRENT KNOWLEDGE ON THE TOPIC?

☑ Rapid enterocyte turnover is a prominent feature of gastrointestinal (GI) tract. Considerable interindividual variability (IIV) in enterocyte lifespan has been reported. A previously developed model of enterocyte turnover could recover the change of pharmacokinetics in populations with altered enterocyte lifespan.

WHAT QUESTION DID THIS STUDY ADDRESS?

☑ Does the enterocyte turnover affect pharmacodynamics (PDs) in the gut wall? If yes, what is the potential impact of IIV in enterocyte lifespan on PDs or optimal dosage regimen?

WHAT DOES THIS STUDY ADD TO OUR KNOWLEDGE?

☑ The enterocyte turnover significantly changes PDs especially when drug-target affinity is strong and the half-life of the target protein is long, which is more significant in the population with shortened enterocyte lifespan. IIV in PDs could occur as a result of IIV in the enterocyte lifespan.

HOW MIGHT THIS CHANGE DRUG DISCOVERY, DEVELOPMENT, AND/OR THERAPEUTICS?

☑ This study highlighted the potential risk of IIV in PDs derived from the IIV in enterocyte lifespan and put the seed of building further mechanistic modeling for treatment of GI diseases when the enterocyte is the pharmacological target.

The gastrointestinal (GI) tract has been the focus of several potential therapeutic targets linked to GI diseases, including metabolic or inflammatory dieases.[1,2] Drugs for GI diseases have been actively developed, but their success rates are not satisfactory, especially in the latter stage of clinical trials.[3] One of the reasons for failure, which is not limited to drugs for GI diseases, is the underestimation of interindividual variability (IIV) in pharmacodynamics (PDs), leading to nonachievement of clinical end points.[4] Identification of factors that cause IIV in PDs maximizes the success rate of drug development through optimization of the dosage regimen in the target population.

Rapid turnover of the enterocytes is a prominent feature of the gut wall compared with other cells and tissues.[5,6] The enterocytes are produced through cell division of progenitor stem cells at the base of the intestinal villi. Matured enterocytes migrate up the crypt-villous axis and are shed from the tip of the villi into the gut lumen. We previously showed that the enterocyte lifespan in humans is 3.48 days (median) along with large IIV (ranging from 1 to 8 days).[7] Furthermore, multiple factors, such as GI diseases or medical treatments, could amplify the IIV of enterocyte lifespan.[8–10]

In the field of systems pharmacology, the terminal half-life of target protein ($t_{1/2,target}$) and drug-target binding rates are

[1]Centre for Applied Pharmacokinetics Research, University of Manchester, Manchester, UK; [2]Laboratory for Safety Assessment and ADME, Pharmaceuticals Research Center, Asahi Kasei Pharma Corporation, Shizuoka, Japan; [3]Logistics and Informatics in Health Care, School of Engineering Sciences in Chemistry, Biotechnology and Health (CBH), KTH Royal Institute of Technology, Stockholm, Sweden; [4]Simcyp Division, Certara UK, Sheffield, UK. *Correspondence: Amin Rostami-Hodjegan (amin.rostami@manchester.ac.uk)

Received: April 1, 2020; accepted: July 16, 2020. doi:10.1002/psp4.12557

recognized as rate-limiting steps of pharmacokinetics (PKs) and/or PDs, and have been incorporated into models to describe the physiology more mechanistically.[11] For example, the target-mediated drug disposition model takes into account the $t_{1/2,target}$ and drug-target binding to explain target occupancy and/or nonlinear PKs.[12] Interestingly, previous studies reported that some proteins or drugs showed $t_{1/2,target}$ or drug-target residence time, a reciprocal of dissociation rate constant (k_{off}), comparable to or longer than enterocyte lifespan.[13–20]

Although the importance of $t_{1/2,target}$ and drug-target binding rates has been discussed, most GI models either ignored the enterocyte turnover or used a lumped cell-protein turnover. Shankaran *et al*. considered only the turnover of epithelial cells in their mechanistic model of chemotherapy-induced diarrhea.[21] The mechanistic PK/PD model for proton pump inhibitors in Sud *et al*. considered both turnover of the intestinal epithelia and target protein, however, these were treated as independent turnover rates and their nesting was ignored.[22] Given comparable parameter range of enterocyte lifespan, $t_{1/2,target}$, and drug-target binding rates, enterocyte turnover is likely to be one of the rate-limiting rates in PDs of enterocyte-targeting drugs. However, no study has considered how often we are missing the impact of enterocyte turnover on PDs of enterocyte-targeting drugs, nor the impact of IIV in enterocyte lifespan on IIV in PDs.

However, the evaluation of these possibilities in actual clinical studies is challenging due to the lack of clinical studies conducted for this purpose. This is an area where model-informed drug development (MIDD) can advance these hypothetical situations.[23,24] Previously, we have shown that the nested-enzyme-within-enterocyte (NEWE) turnover model, which incorporates nested enterocyte and metabolic enzyme turnover, can accurately describe the change in PKs in special populations with altered enterocyte kinetics.[25] Here, we aimed to explore the impact of enterocyte turnover on PDs of enterocyte-targeting drugs by extending the NEWE model to account for PDs. Changes in PDs derived from the IIV in enterocyte lifespan were also investigated through simulations over realistic parameter ranges obtained through a comprehensive literature search. Furthermore, the applicability of the model was assessed in context of approved enterocyte-targeting drugs along with their target sites or kinetic information.

METHODS

The NEWE turnover model for pharmacodynamics

The NEWE model for PDs (NEWE-PD) is based on the original NEWE model structure (**Figure 1a**).[25] The model consists of an oral dose depot, intestinal lumen, enterocytes, lamina propria, liver, and central compartments. The description of the gut wall is presented below, and the details of other compartments and parameter values are given in the **Supplementary Material, Section 1**.

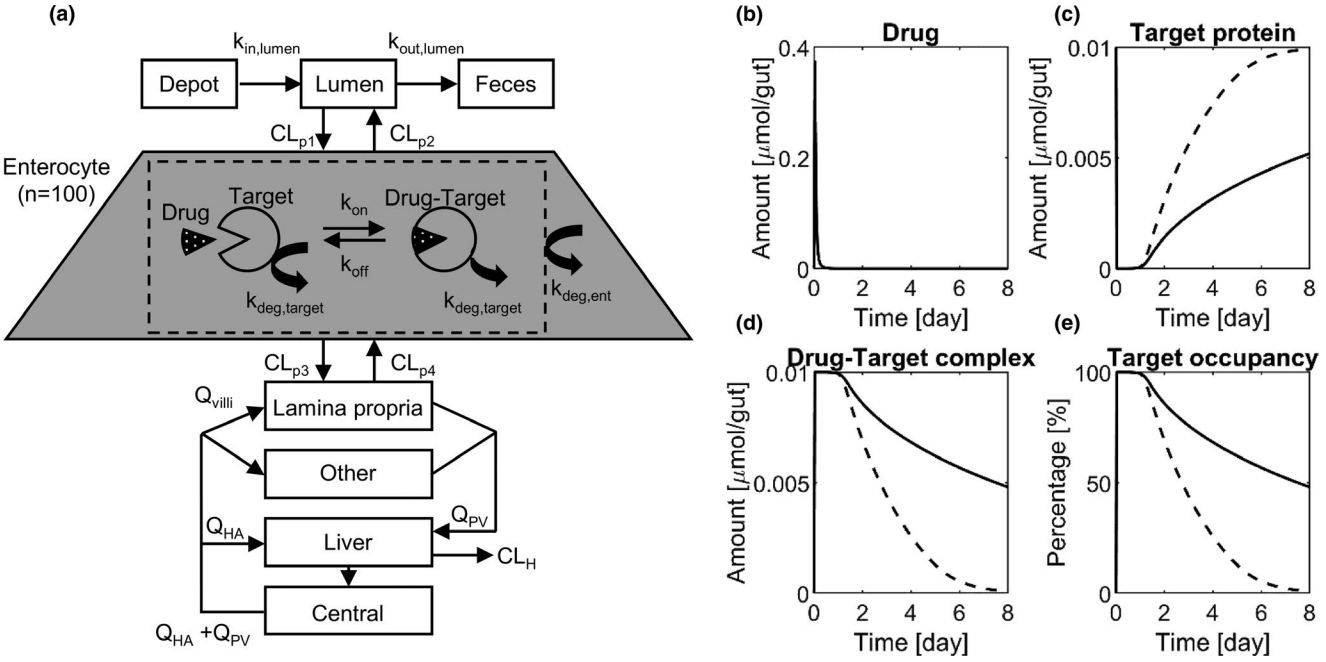

Figure 1 Nested enzyme-within-enterocyte turnover model for pharmacodynamics (PDs). (**a**) Diagram of the nested enzyme-within-enterocyte turnover model for PDs (NEWE-PD). Representative simulations in the NEWE-PD model. Time profiles of (**b**) drug, (**c**) target protein, (**d**) drug-target complex, and (**e**) target occupancy in the whole gut. Solid lines and dashed lines represent simulations without or with enterocyte turnover, respectively. Enterocyte lifespan = 3.48 days, half-life of target protein = 300 hours, k_{on} = 10^2 /nM/h, k_{off} = 10^{-1}/h, and passive permeability of the single membrane = 0.1 cm/h. CL_H, hepatic clearance; CL_{p1-4}, membrane permeability clearance; $k_{deg,ent}$, reciprocal of enterocyte lifespan; $k_{deg,target}$, degradation rate of target protein; $k_{in,lumen}$, gastric emptying rate constant; k_{off}, drug dissociation rate constant; k_{on}, drug association rate constant; $k_{out,lumen}$, small intestine transit; Q_{HA}, blood flow in hepatic artery; Q_{PV}, blood flow in portal vein; Q_{villi}, blood flow in villi.
[Correction added on 4 November 2020 after first publication: The units of two kinetic parameters 'k_{on}' and 'k_{off}' are corrected to /nM/h and /h throughout the article]

Description of the gut wall

The gut wall was modeled as a population of 100 enterocytes as relative ratio uniformly distributed along the crypt-villous axis. Each enterocyte was modeled at four levels: drug amount, drug-target binding, target turnover, and enterocyte turnover. The drug-target binding was expressed by the one-step binding model (Eq. 1); drug (D) binds to target protein (T) at the association rate constant (k_{on}), and drug-target complex (DT) dissociates at the rate of k_{off}.

$$D + T \underset{k_{off}}{\overset{k_{on}}{\rightleftarrows}} \mathrm{DT} \tag{1}$$

Detailed descriptions of protein turnover can be found in our previous report.[25] Briefly, turnover of protein is described by zero-order synthesis ($T_0 \cdot k_{deg}$) and first-order degradation ($T(t) \cdot k_{deg}$), where $T(t)$ is the amount of protein at time t; k_{deg} is the first-order degradation rate constant of protein; and T_0 is the amount of protein at steady-state (Eq. 2).

$$\frac{dT}{dt} = T_0 \cdot k_{deg} - T(t) \cdot k_{deg} \tag{2}$$

Accounting for drug-target binding and target protein turnover, the amount of target protein ($T(t)_i$) and drug–target complex ($DT(t)_i$) in the i^{th} enterocyte at time t are described as follows (Eq. 3 and Eq. 4). The common degradation rate constant ($k_{deg,target}$) was assumed for target protein and drug-target complex.

$$\frac{dT_i}{dt} = k_{off} \cdot \mathrm{DT}(t)_i - k_{on} \cdot T(t)_i \cdot D(t)_{ent,i} - k_{deg,target} \cdot T(t)_i + k_{deg,target} \cdot T_0 \tag{3}$$

$$\frac{dDT_i}{dt} = k_{on} \cdot T(t)_i \cdot D(t)_{ent,i} - k_{off} \cdot \mathrm{DT}(t)_i - k_{deg,target} \cdot \mathrm{DT}(t)_i \tag{4}$$

The drug amount ($D_{ent,i}$) in the i^{th} enterocyte was described as a function of drug-target binding and passive permeation of drug at both sides of the enterocytes (Eqs. 5–7). Other factors, such as active transport, protein binding, or ionization of drug, were not included in this model for simplicity. Influx and efflux membrane permeability clearance at the apical (CL_{p1} and CL_{p2}) and basolateral side of the enterocyte (CL_{p4} and CL_{p3}) were defined as a product of passive permeability of the single membrane (P_{single}) and membrane surface area (S_{apical} and S_{basal}), accounting for microvilli expansion.

$$\mathrm{CL_{p1}} = \mathrm{CL_{p2}} = \frac{P_{single} \cdot S_{apical}}{n\_cells} \tag{5}$$

$$\mathrm{CL_{p3}} = \mathrm{CL_{p4}} = \frac{P_{single} \cdot S_{basal}}{n\_cells} \tag{6}$$

$$\frac{dD_{ent,i}}{dt} = \frac{\mathrm{CL_{p1}} \cdot D(t)_{lumen}}{V_{lumen}} + \frac{\mathrm{CL_{p4}} \cdot D(t)_{propria}}{V_{propria}} - \frac{(\mathrm{CL_{p2}} + \mathrm{CL_{p3}}) \cdot D(t)_{ent,i}}{V_{ent}} - k_{on} \cdot D(t)_{ent,i} \cdot T(t)_i + k_{off} \cdot \mathrm{DT}(t)_i \tag{7}$$

where V_{lumen}, $V_{propria}$, and V_{ent} represent the volumes of the gut lumen, lamina propria, and single enterocyte, respectively; $D(t)_{lumen}$ and $D(t)_{propria}$ represent drug amounts in the lumen and lamina propria compartments at time t, respectively.

Detailed descriptions of enterocyte turnover can also be found in our previous report.[25] In brief, enterocyte turnover was expressed using the cumulative probability of enterocyte turnover (e_i) of the i^{th} enterocyte increased at a rate of $k_{deg,ent}$, which was a reciprocal of enterocyte lifespan (Eq. 8). The probability of turnover at time zero was uniformly distributed between zero and one across the enterocyte population. When $e_i(t)$ reached a value of one, all the dependent variables in the i^{th} enterocyte were reinitialized, namely, e_i, $D_{ent,I}$, and DT_i were initialized to zeros, and T_i was initialized to T_0.

$$\frac{de_i}{dt} = k_{degent} \tag{8}$$

Description of pharmacodynamics

The degree of PDs in the gut wall was defined to be equal to an area under the curve of target occupancy in the whole gut vs. time (AUC_{TO}) (Eq. 9). Relative fold change of AUC_{TO} between the models with and without enterocyte turnover was defined as the contribution index that was used to quantify the contribution of enterocyte turnover on PDs (Eq. 10).

$$\mathrm{AUC_{TO}} \underline{\underline{\mathrm{def}}} \int_0^{\infty} \sum_{i}^{n\_cells} \frac{DT(t)_i}{T(t)_i + DT(t)_i} \tag{9}$$

$$\text{Contribution index} \underline{\underline{\mathrm{def}}} \frac{\mathrm{AUC_{TO}\ in\ the\ simulation\ without\ enterocyte\ turnover}}{\mathrm{AUC_{TO}\ in\ the\ simulation\ with\ enterocyte\ turnover}} \tag{10}$$

Parameter sensitivity analysis

Probability distributions of kinetic parameters in the enterocyte compartment were determined based on literature to ensure realistic parameter ranges in the sensitivity analysis (details in **Supplementary Material, Section 2**). Statistical values of enterocyte lifespan were obtained from the result of a previously reported meta-analysis.[7] The values were obtained from populations including both healthy and patients with GI disease due to the scarcity of data. Probability distributions of $t_{1/2,target}$ and drug-protein binding constants were obtained by integrating multiple data from several references.[13–16,18–20] Lack of reports on $t_{1/2,target}$ of multiple proteins in *in vitro* enterocytes was compensated using $t_{1/2,target}$ in other cell lines, such as hepatocytes. P_{single} were calculated from the apparent permeability determined in Caco-2 assays, and plotted against the fraction absorbed in humans[26] (details in **Supplementary Material, Section 1**). Simulations of contribution index were performed with several combinations of kinetic parameters within plausible parameter ranges as determined in this study.

Virtual clinical study in populations with different enterocyte lifespans

Two theoretical simulations were performed to investigate the impact of IIV in enterocyte lifespan on clinical outcomes: (1) simulation of the target occupancy-time profile over the identified parameter space, and (2) simulation of the optimal dosage interval that achieved a minimum of 50% target occupancy. Each simulation was performed in populations

with different enterocyte lifespan: populations with median and 5th to 95th percentile of enterocyte lifespan, a population with shortened enterocyte lifespan observed in untreated celiac disease (0.25 days),[8] and a population without considering enterocyte lifespan.

Literature search of gastrointestinal disease and enterocyte-targeting drugs

A stepwise literature search was performed to find enterocyte-targeting drugs for which the NEWE-PD model could be applied (details in **Supplementary Material, Section 3**). First, approved drugs for GI diseases were extracted from the Pharmaprojects drug development database (https://pharmaintelligence.informa.com/products-and-services/data-and-analysis/pharmaprojects (June, 2019)). Second, enterocyte-targeting drugs were extracted based on the locations of target proteins. Finally, $t_{1/2,target}$, drug binding constants, and delivery routes of identified enterocyte-targeting drugs were investigated.

RESULTS

The NEWE turnover model for pharmacodynamics

Representative simulation outputs of the drug amount, target protein, drug-target complex, and target occupancy in the whole gut over time are presented in **Figure 1b–e**. Following per oral drug administration, the amount of drug in the enterocyte compartment quickly peaked and returned to the baseline within a few hours. Drug-target complex and target occupancy also reached peak levels quickly but remained elevated after the drug was eliminated from the enterocytes due to the sustained drug-target binding. In the simulation without enterocyte turnover, target occupancy gradually returned to baseline level, which was governed by both drug-target equilibrium and turnover of target protein. The simulation with enterocyte turnover showed faster decline of target occupancy as the dependent variables (drug, target protein, and drug-target complex) in the enterocyte compartments were re-initialized by enterocyte turnover.

Table 1 Probability distributions of kinetics parameters

Parameter	Median (5th–95th percentile)	Number of data	Data source, experimental condition	References
Enterocyte lifespan, days	3.48 (1.69–7.17)	265	Collated enterocyte lifespan in whole intestinal segment (from stomach to colorectal region) in populations including both healthy and GI disease patients	7
Half-life of target protein, hours	58 (12–333)	4,956	*In vitro* study using cryopreserved primary human hepatocyte	14
		5,028	*In vitro* study using NIH3T3 mouse fibroblasts	15
		5,908	*In vitro* study using HeLa cells	16
		2,801	*In vitro* study using primary rat neuron	13
k_{on}, /nM/h	3.7 (3.2×10^{-2}–2.1×10^{2})	35	Binding kinetics constant of FDA-approved drugs for their main target kinases evaluated in kinetic probe competition assays	18
		31	Association constants of agonists, antagonists, and endogenous ligands for GPCRs	19
		32	Collated binding kinetic constants for drugs or drug candidates	20
k_{off}, /h	2.6 (4.3×10^{-2}–2.4×10^{2})	33	Binding kinetics constant of FDA-approved drugs for their main target kinases evaluated in kinetic probe competition assays	18
		31	Dissociation constants of agonists, antagonists, and endogenous ligands for GPCRs	19
		32	Collated binding kinetic constants for drugs or drug candidates	20
k_{d}, nM	1.0 (9.1×10^{-3}–1.5×10^{3})	33	Binding kinetics constant of FDA-approved drugs for their main target kinases evaluated in kinetic probe competition assays	18
		31	Dissociation constants of agonist or antagonist for endogenous ligand for different GPCRs	19
		32	Collated binding kinetic constants for drugs or drug candidates	20

FDA, US Food and Drug Administration; GPCR, G protein-coupled receptor; k_{d}, equilibrium constant; k_{off}, drug dissociation constant; k_{on}, drug association constant.

Parameter sensitivity analysis

Probability distributions of kinetic parameters are summarized in **Table 1**. Representative values or ranges of kinetic parameters used in the parameter sensitivity analysis were determined as follows. Geometric mean of enterocyte lifespan (3.48 days)[3] and shortened enterocyte lifespan observed in untreated coeliac disease (0.25 days)[8] were selected as representative values. The values of $t_{1/2,target}$ were set to 12, 60, and 300 hours to cover 5th percentile, median, and 95th percentile values, respectively. The ranges of k_{on} (10^{-2} to 10^{3} /nM/h) and k_{off} (10^{-2} to 10^{5}/h) were selected to cover the whole parameter space observed. P_{single} of 0.1 and 0.001 cm/h were used as representative values for high-permeable and low-permeable drugs, respectively, based on the correlation between P_{single} and fraction absorbed in humans (**Figure S1**).

Throughout the parameter sensitivity analysis with different combinations of kinetic parameters, a consistent tendency toward an elevation of contribution index was observed; the stronger the drug-target binding (higher k_{on} or lower k_{off}) or the longer the $t_{1/2,target}$ was, the higher the contribution index was (**Figure 2** and **Figure 3**). **Figure 2** shows the simulation results for the high-permeable drug (P_{single} = 0.1 cm/h). At an enterocyte lifespan of 3.48 days, the contribution of enterocyte turnover was negligible for the lowest $t_{1/2,target}$ (12 hours; **Figure 2a**). As $t_{1/2,target}$ increased, the contribution index also increased at specific ranges of binding constants (**Figure 2b,c**). At an enterocyte lifespan of 0.25 days, the contribution indices were higher and spread out over a more extensive parameter space (**Figure 2d–f**). The most extensive increase of contribution index was observed when enterocyte lifespan = 0.25 days and $t_{1/2,target}$ = 300 hours (**Figure 2f**). With the exception of drugs with k_{on} = 10^{-2}/nM/h and k_{off} = 10^{-1}/h, which is discussed in **Supplementary Material, Section 4**, a minimum of twofold increase of contribution index was observed only when equilibrium constant (k_d) was smaller than ~ 1 nM.

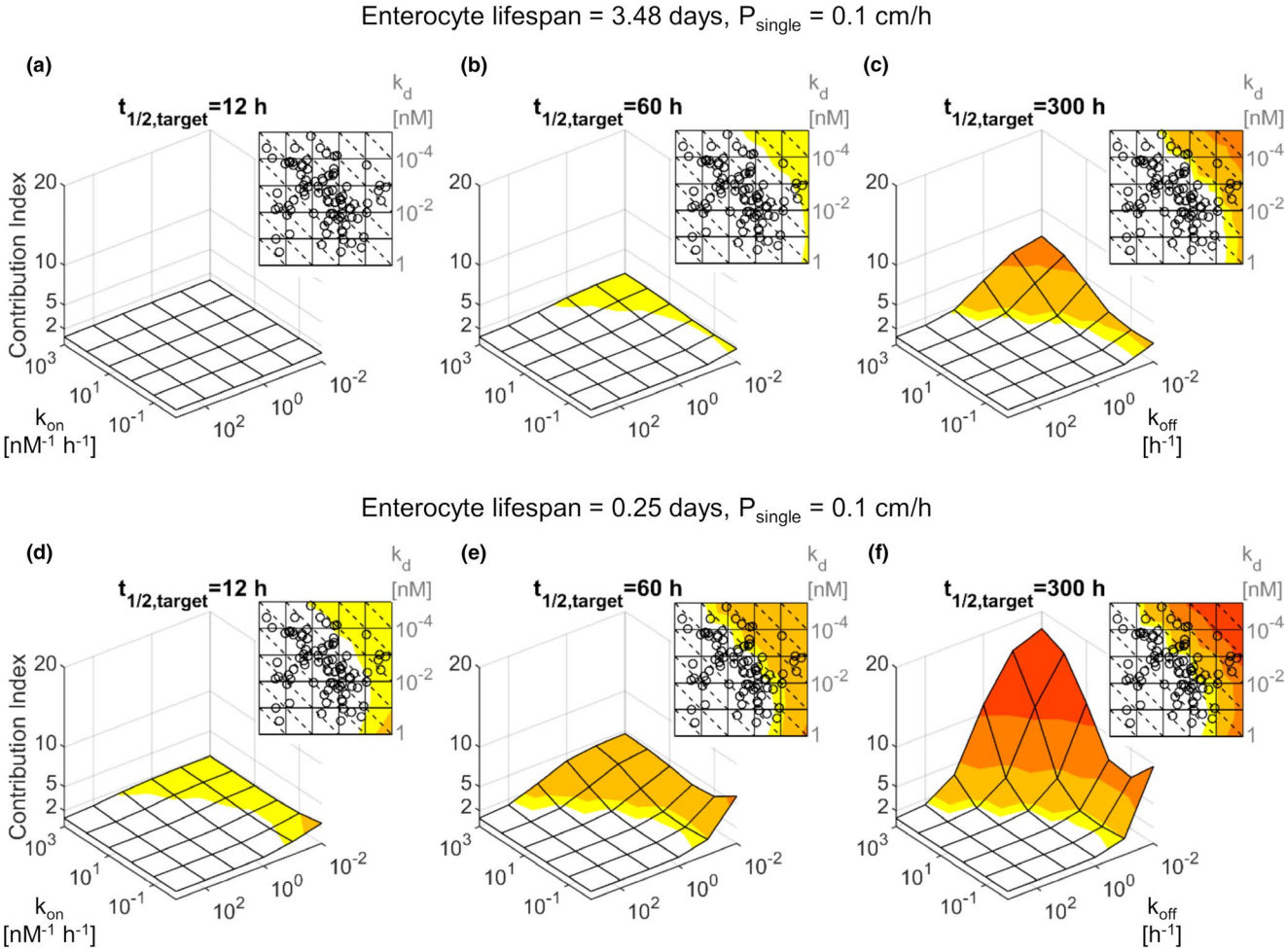

Figure 2 Contribution index simulated for high-permeable drug with varying half-life of target proteins and binding constants. Simulations were performed for high-permeable drug (passive permeability of single membrane (P_{single}) = 0.1 cm/h) with enterocyte lifespan = 3.48 days (**a–c**) or 0.25 days (**d–f**). Heat maps of contribution index were overlayed on top of the scatter plot of binding kinetic constants collated in our literature search, where each dot in the scatter plot represents each drug data and diagonal dashed lines represent equilibrium constant (k_d) (as shown in **Figure S3e**). **a, d** Half-life of target protein ($t_{1/2,target}$) = 12 hours. **b, e** $t_{1/2,target}$ = 60 hours. **c, f** $t_{1/2,target}$ = 300 hours. k_{on}, drug association rate constant; k_{off}, drug dissociation rate constant. Color bar: yellow, 1.5–2; light orange, 2–5; deep orange, 5–10; and red, 10–20.

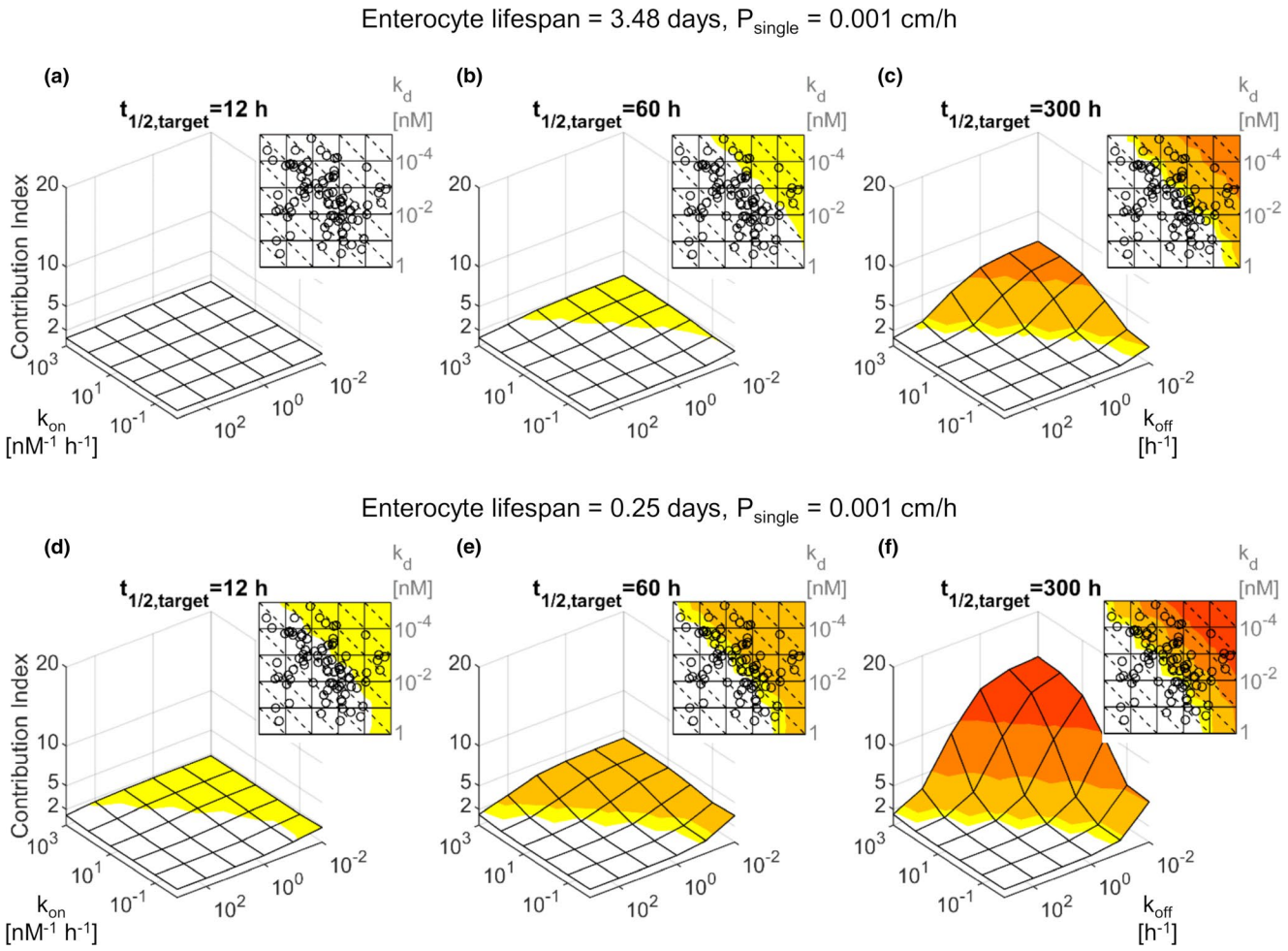

Figure 3 Contribution index simulated for low-permeable drug with varying half-life of target proteins and binding constants. Simulations were performed for low-permeable drug (passive permeability of single membrane (P_{single}) = 0.001 cm/h) with enterocyte lifespan = 3.48 days (**a–c**) or 0.25 days (**d–f**). Heat maps of contribution index were overlayed on top of the scatter plot of binding kinetic constants collated in our literature search, where each dot in the scatter plot represents each drug data and diagonal dashed lines represent equilibrium constant (k_d) (as shown in **Figure S3e**). **a, d** Half-life of target protein ($t_{1/2,target}$) = 12 hours. **b, e** $t_{1/2,target}$ = 60 hours. **c, f** $t_{1/2,target}$ = 300 hours. k_{on}, drug association rate constant; k_{off}, drug dissociation rate constant. Color bar: yellow, 1.5–2; light orange, 2–5; deep orange, 5–10; and red, 10–20.

Figure 3 shows the simulation results for the low-permeable drug (P_{single} = 0.001 cm/h) at an enterocyte lifespan of 3.48 days **(Figure 3a–c)** and 0.25 days **(Figure 3d–f)**. The maximum contribution index was comparable between the low-permeable and high-permeable drugs. However, the contribution index increased over a more extensive parameter space for the low-permeable drugs. The most extensive increase of contribution index was observed when enterocyte lifespan = 0.25 days and $t_{1/2,target}$ = 300 hours, where a minimum of twofold increase of contribution index was again only observed when k_d was smaller than ~ 1 nM **(Figure 3f)**.

These results showed that the increase of contribution index was strongly affected by enterocyte lifespan especially when k_d was smaller than at least 1 nM. It also implied that IIV in enterocyte lifespan may cause IIV in PDs under certain conditions.

Virtual clinical study in populations with different enterocyte lifespans

Target occupancy-time profiles of drugs with several combinations of binding constants were simulated with $t_{1/2,target}$ = 300 hours (95th percentile of $t_{1/2,target}$) and P_{single} = 0.1 cm/h (high-permeable drug). The target occupancy-time profile depended on enterocyte lifespan at specific ranges of binding constants (**Figure 4**). Similar to the results of the sensitivity analysis, the change was more apparent in the population with shortened enterocyte lifespan (0.25 days) than the population with enterocyte lifespan of geometric mean (3.48 days). The change in PDs was also observed in populations with 5th and 95th percentile of enterocyte lifespan (1.69 and 7.17 days, respectively). For instance, approximately twofold difference of AUC_{TO} was observed between the 5th and 95th percentile of AUC_{TO} when k_{on} = 10^2/nM/h and

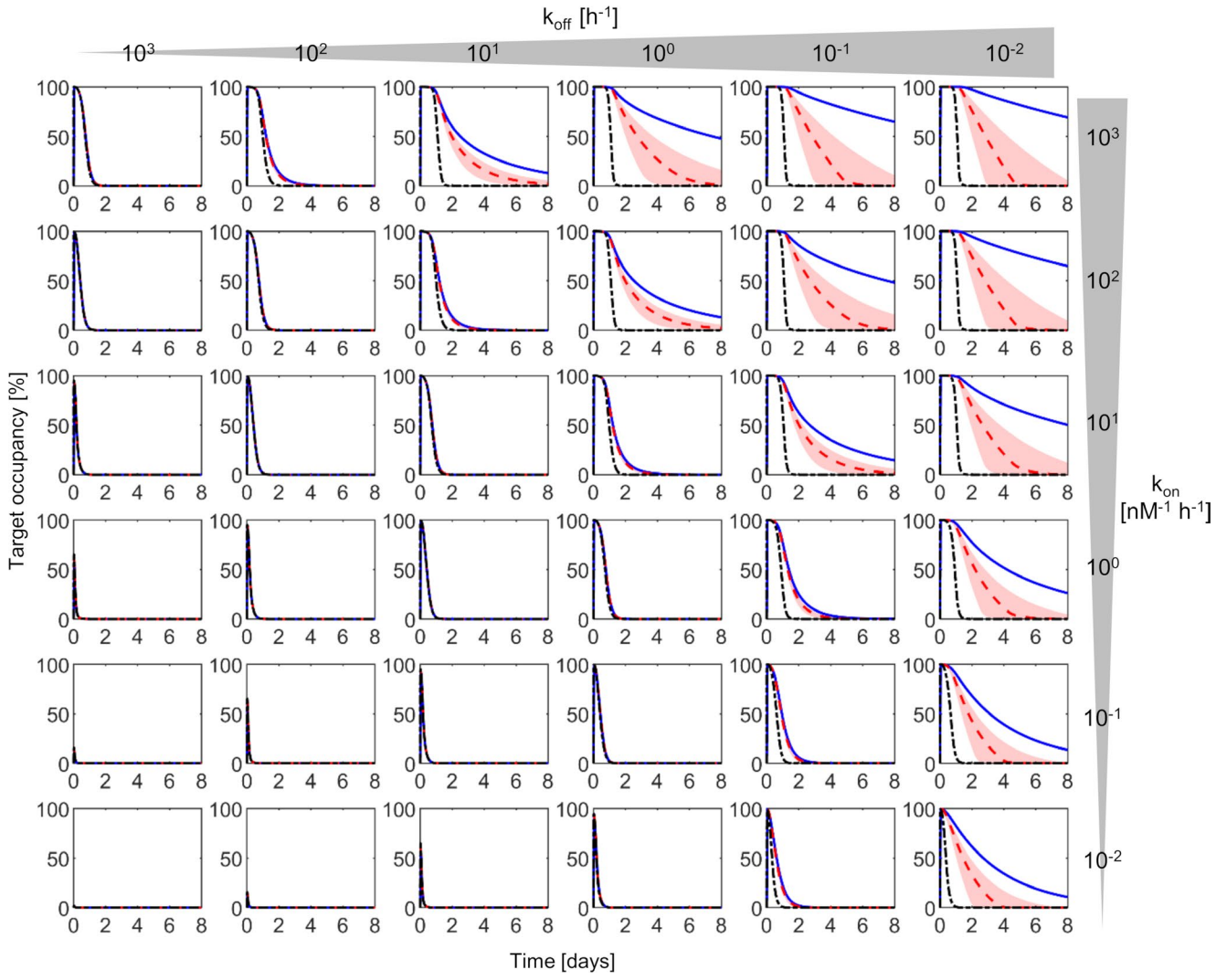

Figure 4 Impact of enterocyte lifespan on target occupancy-time profile. Target occupancy-time profiles of drugs with several combinations of binding constants simulated in virtual populations with different enterocyte lifespans: red dashed line; geometric mean (3.48 days), black dash-dotted line; shortened enterocyte lifespan (0.25 days), red shadow; 5th to 95th percentiles (1.69–7.17 days), and blue solid line; without considering enterocyte turnover. Triangles on the top and right side of figures relative strength of drug binging. k_{on}, drug association rate constant; k_{off}, drug dissociation rate constant. Half-life of target protein = 300 hours and passive permeability of single membrane = 0.1 cm/h.

$k_{off} = 10^{-1}$/h, which were the strongest binding constants found in the collation for kinetic parameters **(Figure S3f)**. Assuming the strongest binding drug, optimal dosage interval to achieve a minimum of 50% target occupancy over 2 weeks also depended on enterocyte lifespan (**Figure 5**). The number of dose administrations differed between populations with shortened enterocyte lifespan (13 times) and with enterocyte lifespan of the geometric mean (6 times) (**Figure 5a,c**), as well as populations at the 5th and 95th percentiles of enterocyte lifespan (7 and 4 times, respectively; **Figure 5b,d**).

Literature search of gastrointestinal disease and enterocyte-targeting drugs

A literature search for GI diseases and corresponding drug treatments was performed to investigate the practical applicability of the NEWE-PD model. The literature search for drugs indicated for GI diseases identified 137 drugs (**Table S3)**, and the follow-up search for the locations of target proteins revealed that 11 drugs of 137 drugs were enterocyte-targeting (**Table 2**). All drugs were formulated for oral delivery and their corresponding $t_{1/2,target}$ varied from 5.7 to 170 hours. The drug-target binding constants were higher than 1 nM except for crofelemer (half of the maximal inhibitory concentration (IC_{50}) = 0.53 nM). The sensitivity analysis showed that the influence of enterocyte turnover became evident only when k_d was smaller than at least 1 nM. Thus, the 10 drugs (apart from crofelemer) were most likely not affected by enterocyte turnover. In addition, short $t_{1/2,target}$ of crofelemer (5.7 hours) suggested that enterocyte turnover is not likely to influence PDs substantially. Here, we substituted IC_{50} or half of maximal effective concentration for binding constants for

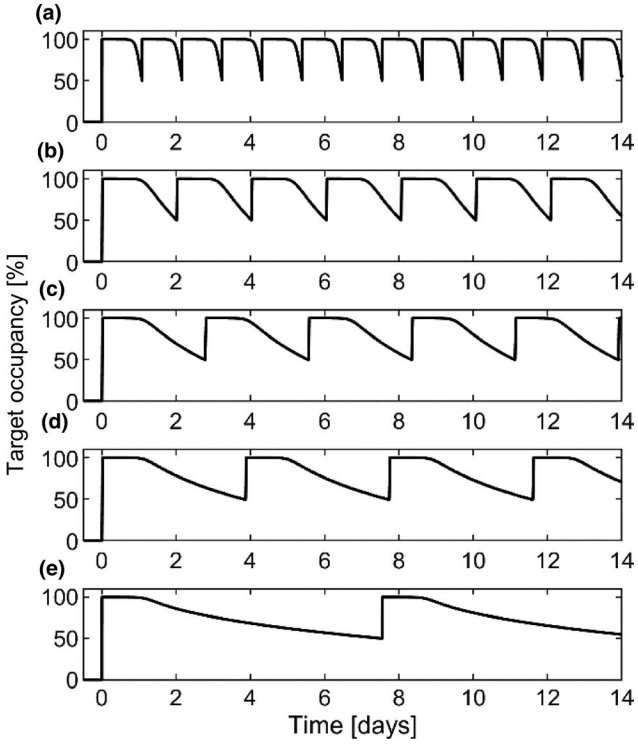

Figure 5 Impact of enterocyte lifespan on optimal dosage interval. Dosage intervals that achieve a minimum of 50% target occupancy over time simulated with different enterocyte lifespans: (**a**) shortened enterocyte lifespan, 0.25 days; (**b**) 5th percentile, 1.69 days; (**c**) geometric mean, 3.48 days; (**d**) 95th percentile, 7.17 days; and (**e**) without enterocyte turnover. Drug association constant = 10^2nM/h, drug dissociation constant = 10/h, and half-life of target protein = 300 hours.

drugs whose binding constants were not reported. Values of IC_{50} and half of maximal effective concentration depend on experimental designs and they can be estimated to be higher than binding constants. Therefore, the NEWE-PD model should be applicable for enterocyte-targeting drugs if their binding constants are below 1 nM.

DISCUSSION

A recent study found that *in vitro* drug potency does not necessarily predict *in vivo* benefit, discussing that the source of this *in vitro-in vivo* discrepancy in PDs appeared to be *in vivo* biology, such as wide variability of target kinetic.[27] One important biology missing here, in the case of enterocyte-targeting drugs, is turnover of enterocytes. Despite its rapid turnover rate comparable to $t_{1/2,target}$ and drug-target binding rates,[13–16,18–20] the impact of enterocyte turnover, as well as its IIV, on PDs of enterocyte-targeting drugs has not been focused solely because it slipped off from our attention without justification. Because such a hypothetical question is an area where MIDD exerts its true potential,[23,24] we explored the potential impact of enterocyte turnover on the PDs by extending the existing enterocyte turnover model for PDs.[25]

The NEWE-PD model was developed by adding the following features to the original model[25]: (1) PD motif; the one-step binding model was used to express drug-target binding, and target occupancy was used as an index of PDs. In addition to target turnover, degradation of drug-target complex was assumed as per the target-mediated drug disposition model.[12] We also assumed that the same degradation rate for both target protein and drug-target complex, resulting in the constant total amount of target protein (sum of target protein and drug-target complex).[28] (2) Bidirectional membrane permeation of the enterocytes. In contrast to most intestinal models assuming unidirectional drug absorption from the intestinal lumen to systemic circulation, several recent models incorporated bidirectional membrane permeability on both sides of the enterocytes to more accurately describe drug absorption.[26] The NEWE-PD model used bidirectional passive permeation to ensure that it was applicable for multiple dosage routes apart from oral drug administration.

Use of realistic parameter ranges, even though they are collected under some assumptions to compensate for the scarcity of data, should ensure some reliability of this theoretical simulation study. Statistical parameters of enterocyte lifespan were calculated using all the data obtained from whole segment of intestine (from stomach to colon) in populations including both healthy patients and patients with colorectal cancer.[3] The influence of regional difference or disease state on IIV in enterocyte lifespan is inconclusive. A recent study evaluated $t_{1/2,target}$ of multiple proteins in *in vivo* murine epithelial cells, with reported median and 5th–95th percentiles of 94 and 77–122 hours, respectively.[17] However, these data were not used in this study because the study ignored the influence of enterocyte turnover, potentially underestimating $t_{1/2,target}$ of some proteins with long $t_{1/2,target}$. Due to the lack of $t_{1/2,target}$ in the *in vitro* enterocytes, $t_{1/2,target}$ in other cell lines were used not to miss proteins with long $t_{1/2,target}$.[10–13] This assumption is not likely to affect the results as the cutoff k_d value of 1 nM was consistent in parameter sensitivity analysis with the wider range of $t_{1/2,target}$ (1–1,000 hours; **Figure S5**).

Throughout the sensitivity analysis, elevated contribution indices were observed when (1) drug-target binding was strong, (2) $t_{1/2,target}$ was long, (3) enterocyte lifespan was short, or (4) membrane permeability was low. The contribution index increases when the enterocyte turnover rate is relatively faster than the decline in target occupancy (**Figure 4**). Because the total amount of target protein (sum of target protein and drug-target complex) is constant over time under the assumption that degradation rates of target protein and drug-target complex are the same, target occupancy changes in proportion to drug-target complex (Eq. 9).[28] The sustained drug-target binding due to the strong drug-target binding or slow replacement of the complex due to the longer $t_{1/2,target}$ leads to the prolonged formation of drug-target complex, making the model more sensitive to enterocyte turnover. Short enterocyte lifespan accelerates the decline of drug-target complex by re-initializing enterocyte compartments more rapidly. High sensitivity of low-permeable drug to enterocyte turnover can be explained by drug rebinding[29]; drugs that dissociate from target proteins rebind to neighboring target proteins when drug diffusion at

Table 2 Gastrointestinal diseases and therapeutic drugs

Disease	Drug	Target protein	Delivery Route	Half-life of target protein, hours	Binding constant, nM	References
Irritable bowel syndrome constipation	Linaclotide	Guanylate cyclase 2C receptor	Oral	37	1.23–1.64 (k_i)	33,34
Irritable bowel syndrome constipation	Plecanatide	Guanylate cyclase 2C receptor	Oral	37	190 (EC_{50})	34,35
Irritable bowel syndrome constipation	Lubiprostone	Chloride channel protein 2	Oral	41	10.5 (k_d)	36,37
Diarrhea	Crofelemer	Cystic fibrosis transmembrane regulator chloride channel Anoctamin 1	Oral Topical	28.2 98	7,000 (IC_{50}) 6,500 (IC_{50})	38–42
Constipation	Elobixibat	Ileal bile acid transporter	Oral	5.7	0.53 (IC_{50})	43,44
Diabetes	Acarbose	Alpha glucosidase	Oral	28–116	> 5.7 (k_i)	45,46
Diabetes	Miglitol	Alpha glucosidase	Oral	28–116	> 87 (k_i)	45,46
Diabetes	Voglibose	Alpha glucosidase	Oral	28–116	> 21 (k_i)	45,46
Hypercholesterolemia	Ezetimibe	Niemann-Pick C1-like 1 protein	Oral	20	200 (k_i)	1,47
Hypercholesterolemia	Lomitapide	Microsomal triglyceride transfer protein	Oral	71–170	8 (IC_{50})	1,48
Hypercholesterolemia	Melinamide	Sterol O-acyltransferase	Oral	8–28	35 (IC_{50})	49,50

EC_{50}, half of maximal effective concentration; FDA, US Food and Drug Administration; GI, gastrointestinal; GPCR, G protein-coupled receptor; IC_{50}, half of the maximal inhibitory concentration; k_d, equilibrium constant; k_i, inhibitory constant; k_{off}, drug dissociation constant; k_{on}, drug association constant.

the site of drug-target binding is restricted, resulting in prolonged formation of drug-target complex. In the NEWE-PD model, enterocyte membranes work as barriers that form a microcompartment preventing drug diffusion. The influence of drug rebinding was more prominent for low-permeable drugs due to higher membrane resistance (**Figure S6**).

Target occupancy-time profile and optimal dose interval significantly differed depending on enterocyte lifespan when drug binding was strong and $t_{1/2,target}$ was long (**Figure 4** and **Figure 5**). The simulations showed altered PDs, not only in populations with extremely short enterocyte lifespan observed in untreated celiac disease,[8] but also in other populations based on its estimated IIV.[7] The US Food and Drug Administration has warned in their draft guidance regarding the diversity of clinical trial populations that the unnecessary exclusion of subjects in early stages of clinical studies may lead to unexpected IIV in large-scale clinical studies.[30] IIV in enterocyte turnover could be relevant in the case populations with altered enterocyte lifespan are not included in the early clinical studies. Individualized dosage regimens based on enterocyte lifespan may overcome this potential problem, but evaluation of individual's enterocyte lifespan with an authentic approach using radioactive compounds is unrealistic in actual clinical trials. Diagnostic evaluation of enterocyte lifespan using potential biomarkers of enterocyte turnover may enable the translation from early to late stage of clinical trials in terms of IIV in PDs.[31]

Out of the 137 drugs for GI diseases identified in this study, only 11 drugs were enterocyte-targeting. The sensitivity analysis showed that the impact of enterocyte turnover on PDs can be significant for drugs with high target affinity (k_d < 1 nM), whereas most of enterocyte-targeting drugs have higher k_d values than 1 nM. Therefore, we can conclude that the enterocyte turnover has little influence on PDs of currently approved enterocyte-targeting drugs due to their relatively weak target affinity. This result was surprising because the binding constants of enterocyte-targeting drugs were found only in the higher half of the parameter distribution of k_d, which was established based on reported data of non-enterocyte-targeting drugs (**Table 1**). The cause of this bias is unknown, but our result may propose a possible interpretation; enterocyte-targeting drugs with high target affinity could have a risk of large IIV in PDs, especially in populations with altered enterocyte lifespan, which can become prominent in the late stage of clinical trials. The weaker the target affinity is, the smaller the IIV in PDs could be based on this hypothesis. However, the other side of the coin would be the risk of clinical trial failure due to inadequate efficacy. The NEWE-PD model could be a useful tool for evaluating the balance between efficacy and IIV of enterocyte-targeting drugs.

A remaining challenge in this study is the validity of the developed model. A previous iteration of the PK module in the NEWE-PD model was validated in our previous study, where the NEWE model appeared to outperform the conventional approach for predicting disease effects on oral absorption.[25] On the other hand, the validation of the PD module, which was added in this study, was difficult due to the lack of enterocyte-targeting drugs to which the NEWE-PD model is applicable. This limitation should be addressed by re-evaluating the PD module for enterocyte-targeting drugs with the following features developed in the future. (1) Drugs with high target affinity, the cutoff of k_d (< 1 nM) can be a criterion in the selection of drugs. (2) Drugs for target proteins with long $t_{1/2,target}$, where the influence of enterocyte turnover is likely to be the case when $t_{1/2,target}$ is several hundred hours (**Figure 2** and **Figure 3**).

The reported $t_{1/2,target}$ of > 3,000 proteins in murine epithelial cells is helpful to find out $t_{1/2,target}$ of target proteins.[17] (3) Drugs targeting diseases with shortened enterocyte lifespan. In addition to untreated celiac disease,[8] altered enterocyte turnover was also observed in other conditions, such as GI mucositis.[9,10] GI cancer shows abnormal cell proliferation.[32] Although GI cancer was excluded from this study because overgrowth of cancer cells was beyond our scope, additional model extension may enable the application of the model for the disease. (4) Drugs targeting other tissues with short lifespan. Short lifespan is also observed in other tissues, such as bone marrow (3.2 days) or cervix (5.7 days).[5] The description of nested turnover in the NEWE-PD models could be extended for these cases.

In conclusion, a mechanistic PK/PD model of the gut wall, accounting for the nested turnover of enterocyte and PD targets, was developed. This model should be considered as a part of the effort toward optimization and rationalization of decisions involved in selection of candidate drugs and plans for investigating their effects through the MIDD approach. The recent reports by the regulatory scientists from leading agencies and other key opinion leaders are all encouraging the wider use of such strategies.[23,24] In many areas, the framework for application of these strategies are still lacking. We hope the current investigation plants the seed of building further mechanistic modeling for treatment of GI diseases when the gut wall is the site of pharmacological target.

Supporting Information. Supplementary information accompanies this paper on the *CPT: Pharmacometrics & Systems Pharmacology* website (www.psp-journal.com).

Funding. The performed analysis was financially supported by a fellowship grant from Asahi Kasei Pharma Corporation.

Conflict of Interest. The authors declared no competing interests for this work.

Author Contributions. H.T., A.S.D., A.A., and A.R.-H. wrote the manuscript. H.T., A.S.D., A.A., and A.R.-H. designed the research. H.T. performed the research. H.T. analyzed the data.

1. Filipski, K.J. *et al*. Intestinal targeting of drugs: rational design approaches and challenges. *Curr. Top. Med. Chem.* **13**, 776–802 (2013).
2. Coskun, M., Vermeire, S. & Nielsen, O.H. Novel targeted therapies for inflammatory bowel disease. *Trends Pharmacol. Sci.* **38**, 127–142 (2017).
3. Thomas, D.W.*et al.*Clinical development success rates 2006–2015. https://www.bio.org/sites/default/files/Clinical Development Success Rates 2006-2015 - BIO, Biomedtracker, Amplion 2016.pdf (2016). Accessed May 29, 2020.
4. Vegvari, C. *et al*. Using clinical trial simulators to analyse the sources of variance in clinical trials of novel therapies for acute viral infections. *PLoS One* **11**, 1–18 (2016).
5. Richardson, R.B., Allan, D.S. & Le, Y. Greater organ involution in highly proliferative tissues associated with the early onset and acceleration of ageing in humans. *Exp. Gerontol.* **55**, 80–91 (2014).
6. Williams, J.M. *et al*. Epithelial cell shedding and barrier function: a matter of life and death at the small intestinal villus tip. *Vet. Pathol.* **52**, 445–455 (2015).
7. Darwich, A.S., Aslam, U., Ashcroft, D.M. & Rostami-Hodjegan, A. Meta-analysis of the turnover of intestinal epithelia in preclinical animal species and humans. *Drug Metab. Dispos.* **42**, 2016–2022 (2014).
8. Brigic, E., Hadzic, D. & Mladina, N. Early and correct diagnosis of celiac disease in the prevention of growth disorders and child development. *Mater. Socio Medica* **24**, 242 (2012).
9. Williamson, R.C., Bauer, F.L., Ross, J.S. & Malt, R.A. Intestinal adaptation (first of two parts). Structural, functional and cytokinetic changes. *N. Engl. J. Med.* **298**, 1393–1402 (1978).
10. Keefe, D.M., Brealey, J., Goland, G.J., Cummins, A.G. Chemotherapy for cancer causes apoptosis that precedes hypoplasia in crypts of the small intestine in humans. *Gut* **47**, 632–637 (2000).
11. Mager, D.E. & Kimko, H.H.C. Systems Pharmacology and Pharmacodynamics (AAPS Advances in the Pharmaceutical Sciences Series), 1st edn. (Springer, Cham, Switzerland, 2016).
12. Mager, D.E. & Jusko, W.J. General pharmacokinetic model for drugs exhibiting target-mediated drug disposition. *J. Pharmacokinet. Pharmacodyn.* **28**, 507–532 (2001).
13. Cohen, L.D. *et al*. Metabolic turnover of synaptic proteins: kinetics, interdependencies and implications for synaptic maintenance. *PLoS One* **8**, e63191 (2013).
14. Mathieson, T. *et al*. Systematic analysis of protein turnover in primary cells. *Nat. Commun.* **9**, 689 (2018).
15. Schwanhüusser, B. *et al*. Global quantification of mammalian gene expression control. *Nature* **473**, 337–342 (2011).
16. Boisvert, F.-M. *et al*. A quantitative spatial proteomics analysis of proteome turnover in human cells. *Mol. Cell. Proteomics* **11**, 1–15 (2012).
17. Arike, L. *et al*. Protein turnover in epithelial cells and mucus along the gastrointestinal tract is coordinated by the spatial location and microbiota. *Cell Rep.* **30**, 1077–1087.e3 (2020).
18. Georgi, V. *et al*. Binding kinetics survey of the drugged kinome. *J. Am. Chem. Soc.* **140**, 15774–15782 (2018).
19. Strasser, A., Wittmann, H.J. & Seifert, R. Binding kinetics and pathways of ligands to GPCRs. *Trends Pharmacol. Sci.* **38**, 717–732 (2017).
20. Dahl, G. & Akerud, T. Pharmacokinetics and the drug-target residence time concept. *Drug Discov. Today* **18**, 697–707 (2013).
21. Shankaran, H. *et al*. Systems pharmacology model of gastrointestinal damage predicts species differences and optimizes clinical dosing schedules. *CPT Pharmacometrics Syst. Pharmacol.* **7**, 26–33 (2018).
22. Sud, D., Joseph, I.M. & Kirschner, D. Predicting efficacy of proton pump inhibitors in regulating gastric acid secretion. *J. Biol. Syst.* **12**, 1–34 (2004).
23. Marshall, S.F. *et al*. Good practices in model-informed drug discovery and development: practice, application, and documentation. *CPT Pharmacometrics Syst. Pharmacol.* **5**, 93–122 (2016).
24. Wang, Y. *et al*. Model-informed drug development: current US regulatory practice and future considerations. *Clin. Pharmacol. Ther.* **105**, 899–911 (2019).
25. Darwich, A.S., Burt, H.J. & Rostami-Hodjegan, A. The nested enzyme-within-enterocyte (NEWE) turnover model for predicting dynamic drug and disease effects on the gut wall. *Eur. J. Pharm. Sci.* **131**, 195–207 (2019).
26. Gertz, M., Harrison, A., Houston, J.B. & Galetin, A. Prediction of human intestinal first-pass metabolism of 25 CYP3A substrates from in vitro. *Clear. Permeability Data* **38**, 1147–1158 (2010).
27. Jansson-Löfmark, R., Hjorth, S. & Gabrielsson, J. Does in vitro potency predict clinical efficacious concentrations? *Clin. Pharmacol. Ther.* 108, 298–305 (2020).
28. Peletier, L.A. & Gabrielsson, J. Dynamics of target-mediated drug disposition. *Eur. J. Pharm. Sci.* **38**, 445–464 (2009).
29. Vauquelin, G. Rebinding: or why drugs may act longer in vivo than expected from their in vitro target residence time. *Expert Opin. Drug Discov.* **5**, 927–941 (2010).
30. Enhancing the diversity of clinical trial populations — Eligibility criteria, enrollment practices, and trial designs guidance for industry | FDA. <https://www.fda.gov/regulatory-information/search-fda-guidance-documents/enhancing-diversity-clinical-trial-populations-eligibility-criteria-enrollment-practices-and-trial>(2019). Accessed May 29, 2020.
31. Crenn, P. *et al*. Plasma citrulline: a marker of enterocyte mass in villous atrophy-associated small bowel disease. *Gastroenterology* **124**, 1210–1219 (2003).
32. Davies, R.J., Miller, R. & Coleman, N. Colorectal cancer screening: prospects for molecular stool analysis. *Nat. Rev. Cancer* **5**, 199–209 (2005).
33. Rappaport, J.A. & Waldman, S.A. The guanylate cyclase C-cGMP signaling axis opposes intestinal epithelial injury and neoplasia. *Front. Oncol.* **8**, 299 (2018).
34. Shailubhai, K. *et al*. Plecanatide and dolcanatide, novel guanylate cyclase-C agonists, ameliorate gastrointestinal inflammation in experimental models of murine colitis. *World J. Gastrointest. Pharmacol. Ther.* **6**, 213–222 (2015).
35. Rao, S.S.C. Plecanatide: a new guanylate cyclase agonist for the treatment of chronic idiopathic constipation. *Therap. Adv. Gastroenterol.* **11**, 1–14 (2018).
36. Joo, N.S., Wine, J.J. & Cuthbert, A.W. Lubiprostone stimulates secretion from tracheal submucosal glands of sheep, pigs, and humans. *Am. J. Physiol. Lung Cell. Mol. Physiol.* **296**, L811–L824 (2009).
37. Jakab, R.L., Collaco, A.M. & Ameen, N.A. Lubiprostone targets prostanoid signaling and promotes ion transporter trafficking, mucus exocytosis, and contractility. *Dig. Dis. Sci.* **57**, 2826–2845 (2012).
38. Tradtrantip, L., Namkung, W. & Verkman, A.S. Crofelemer, an antisecretory antidiarrheal proanthocyanidin oligomer extracted from Croton lechleri, targets two distinct intestinal chloride channels. *Mol. Pharmacol.* **77**, 69–78 (2010).

39. Fisher, J.T. *et al*. Comparative processing and function of human and ferret cystic fibrosis transmembrane conductance regulator. *J. Biol. Chem.* **287**, 21673–21685 (2012).
40. Lukacs, G.L. *et al*. The delta F508 mutation decreases the stability of cystic fibrosis transmembrane conductance regulator in the plasma membrane. Determination of functional half-lives on transfected cells. *J. Biol. Chem.* **268**, 21592–21598 (1993).
41. Oh, U. & Jung, J. Cellular functions of TMEM16/anoctamin. *Pflugers Arch. Eur. J. Physiol.* **468**, 443–453 (2016).
42. Thiagarajah, J.R. & Verkman, A.S. Chloride channel-targeted therapy for secretory diarrheas. *Curr. Opin. Pharmacol.* **13**, 888–894 (2013).
43. Xia, X. *et al*. Degradation of the apical sodium-dependent bile acid transporter by the ubiquitin-proteasome pathway in cholangiocytes. *J. Biol. Chem.* **279**, 44931–44937 (2004).
44. Jiang, C., Xu, Q., Wen, X. & Sun, H. Current developments in pharmacological therapeutics for chronic constipation. *Acta Pharm. Sin. B* **5**, 300–309 (2015).
45. Krentz, A.J. & Bailey, C.J. Oral antidiabetic agents: current role in type 2 diabetes mellitus. *Drugs* **65**, 385–411 (2005).
46. Seibule (Miglitol) tablet interview form. <https://med.skk-net.com/supplies/products/item/SBL_if.pdf> (2017). Accessed May 29, 2020.
47. Pfefferkorn, J.A. *et al*. Substituted oxazolidinones as novel NPC1L1 ligands for the inhibition of cholesterol absorption. *Bioorg. Med. Chem. Lett.* **18**, 546–553 (2008).
48. Sulsky, R. *et al*. 5-Carboxamido-1,3,2-dioxaphosphorinanes, potent inhibitors of MTP. *Bioorg. Med. Chem. Lett.* **14**, 5067–5070 (2004).
49. Kusunoki, J., Aragane, K., Yamaura, T. & Ohnishi, H. Studies on acyl-CoA: cholesterol acyltransferase (ACAT) inhibitory effects and enzyme selectivity of F-1394, a pantotheic acid derivative. *Jpn. J. Pharmacol.* **67**, 195–203 (1995).
50. Iqbal, J. & Hussain, M.M. Intestinal lipid absorption. *Am. J. Physiol. Endocrinol. Metab.* **296**, 1183–1194 (2009).